Received: 16 August 2021 | Revised: 16 November 2021 | Accepted: 27 November 2021

DOI: 10.1002/ldr.4161

RESEARCH ARTICLE

WILEY

Are compacted tramlines underestimated features in soil erosion modeling? A catchment-scale analysis using a process-based soil erosion model

Philipp Saggau | **Michael Kuhwald** | **Wolfgang Berengar Hamer** | **Rainer Duttmann**

Department of Geography, Christian-Albrechts-University of Kiel, Kiel, Germany

Correspondence
Philipp Saggau, Department of Geography, Christian-Albrechts-University of Kiel, Ludewig-Meyn Straße 08, Kiel, 24118 Germany
Email: saggau@geographie.uni-kiel.de

Funding information
Federal Ministry of Education and Research (within the BonaRes Framework), Grant/Award Number: 031B0684C

Abstract

Process-based model ling has long been used as a well-suited tool to simulate soil erosion. Despite a large number of scientific articles that emphasize the role of compacted tramlines for soil erosion and surficial nutrient transport, no study exists that integrates these artificial structures into process-based modelling at catchment scales. Thus, this study aims to quantify the effects of tramline compaction on soil erosion dynamics within a catchment. For this reason, high-resolution spatial data (1 × 1 m) have been incorporated into the model EROSION 3D, which was used, calibrated, and tested for a soil erosion event with measured discharge and soil loss data. To quantify the contribution of tramlines to soil erosion, two different model parameterizations have been used: the tramline parameterization (TLP) and the common model parameterization (CP) that disregards the tramlines. The results reveal that: (i) the parameterization of tramlines improved model outcomes; (ii) tramlines significantly contribute to overall soil loss and sediment entrance into the channel network; (iii) the bulk density of tramlines is the most important driver of increases in soil erosion and runoff. Moreover, our investigation suggests that the impact of compacted tramlines have long been underestimated in soil erosion modelling and can assist in the assessment of surficial flow path connectivity. Thus, the integration of tramlines into soil erosion modeling is important for the implementation of adequate soil conservation and water protection measures.

KEYWORDS
physical-based model, soil compaction, soil degradation, water erosion, wheel tracks

1 | INTRODUCTION

Soil erosion by water is acknowledged as a primary concern in the degradation of soil quality and functionality (Borrelli et al., 2016; Lal, 2014). The reduction of soil productivity by erosional loss challenges sustainable soil management around the globe (Pennock, 2019; Poesen, 2018), while the redistribution of soil particles and nutrients causes a variety of negative impacts in adjacent ecosystems (Boardman & Poesen, 2006; Fiener et al., 2011; Poesen, 2018). Soil erosion also produces additional economic costs

for farmers, for example, due to increased fertilizer application, which has been estimated at 115 billion US$ for N and P fertilizer annually (Govers et al., 2017).

Several monitoring and field experiments across Europe identified that frequent and severe soil erosion is commonly linked to tramlines and tractor wheeling (e.g., Evans, 2017; Prasuhn, 2020; Remund et al., 2021; Steinhoff-Knopp & Burkhard, 2018). Tramlines are semi-permanent structures established by farm machinery for crop maintenance. Depending on the operating distance, tyre, and axle width, tramlines are estimated to occupy 3% (Gillespie & McDonnell, 2020) to 6% (Augustin et al., 2020) of arable fields. Despite the low area percentage, Evans (2017) observed that 70% of 788 erosion events occurred in tramlines. The increased susceptibility of tramlines to soil erosion can be linked to an increased runoff generation due to soil compaction, the concave micro-relief of tyre ruts and to the absence of vegetation cover (Fleige & Horn, 2000; Gillespie & McDonnell, 2020; Withers et al., 2006) as shown in Figure 1. In addition, previous studies reported that losses of P from tramlines are significantly higher compared to areas without tramlines (Deasy et al., 2009; Silgram et al., 2010; Withers et al., 2006). Based on monitoring Remund et al. (2021) concluded that tramlines belong to the most important pathways of sediment and particulate phosphorus, for example, into water bodies. A consideration of the effects of tramlines on soil erosion processes seems to be essential to identifying at-risk areas and surficial pathways for water and sediment transport on arable soils accurately.

Today soil erosion models are indispensable tools for predicting at-risk areas and estimating soil loss rates beforehand and, in a cost-, and time-efficient manner (Jetten et al., 2003; Schindewolf et al., 2012). Despite the variety of qualitative and quantitative soil erosion models currently available (Batista et al., 2019; Merritt et al., 2003), tramlines are rarely given explicit consideration in soil erosion modelling (e.g., PSYCHIC, Davison et al., 2008), although raster-based models generally have the capability to account for small-scale structures by adjusting the cell-sizes (Baartman et al., 2020).

A first attempt to integrate high spatial resolution data of tramline wheeling into a raster- and process-based model, EROSION 3D (E3D), was shown by Saggau et al. (2019). They incorporated tramline properties in the parameterization process and tested the effects of different spatial resolutions on soil loss and runoff for three different fields. It was found adjusting the input parameters for tramlines in E3D improves the relative prediction accuracy for cell sizes of ≤1 m. However, the modeling results were critical as the study lacked adequate calibration, which led to an over-prediction of soil erosion rates by two orders of magnitude. Simultaneously, modeled surface runoff in tramlines was underestimated, as the parameterization did not account for tyre ruts. Finally, the limited spatial extent of individual fields could not deliver suitable information regarding the fate of mobilized sediments and surface runoff beyond field borders.

Until now, no process-based model approach exists that analyses the effects of tramlines on soil erosion dynamics and sediment delivery to surface waters for an entire catchment. Thus, our study aimed to conduct a catchment-scale analysis that includes the spatial patterns and properties of tramlines using the process-based soil erosion model E3D for a single erosion event. The objectives of this study are: (i) to improve the predictive accuracies of soil loss and runoff by conducting model calibration and optimizing the parameterization process, by accounting for tyre ruts; (ii), to evaluate the impact of tramlines on soil erosion, runoff dynamics and sediment transfer; and (iii) to identify the driving parameters of tramlines that affect soil erosion and surface runoff dynamics. We hypothesize that: (1) tramlines are the main contributor to runoff generation and soil loss within a catchment; (2) the integration of tramlines improves model outcomes; and (3) soil compaction is the driving parameter responsible for soil loss and runoff generation in tramlines.

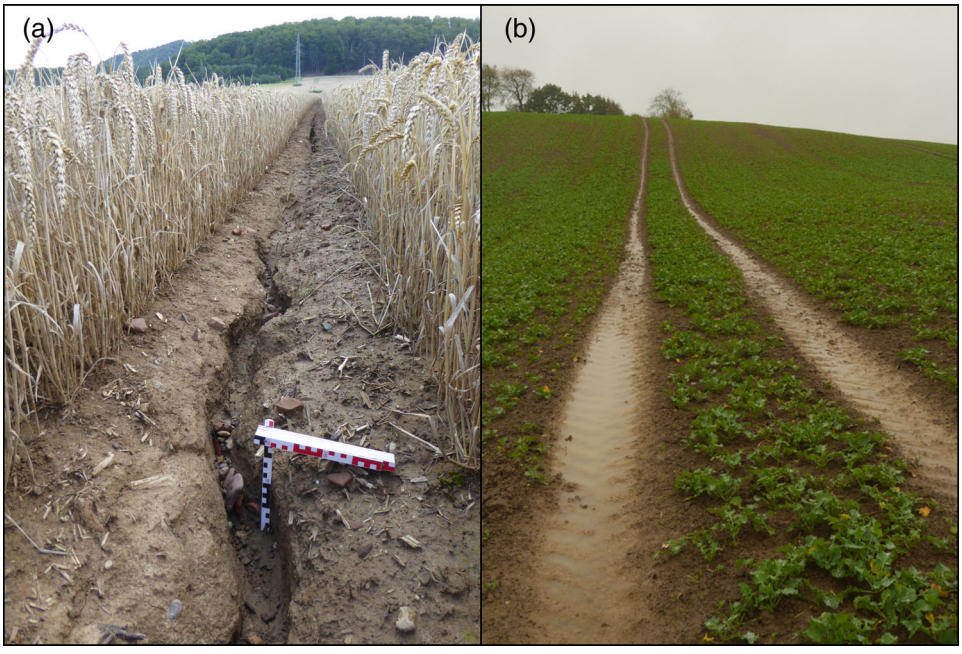

FIGURE 1 Rill erosion (a; Leibniz University of Hannover, 2021) and surface runoff (b; Saggau, 2017) within compacted tramlines [Colour figure can be viewed at wileyonlinelibrary.com]

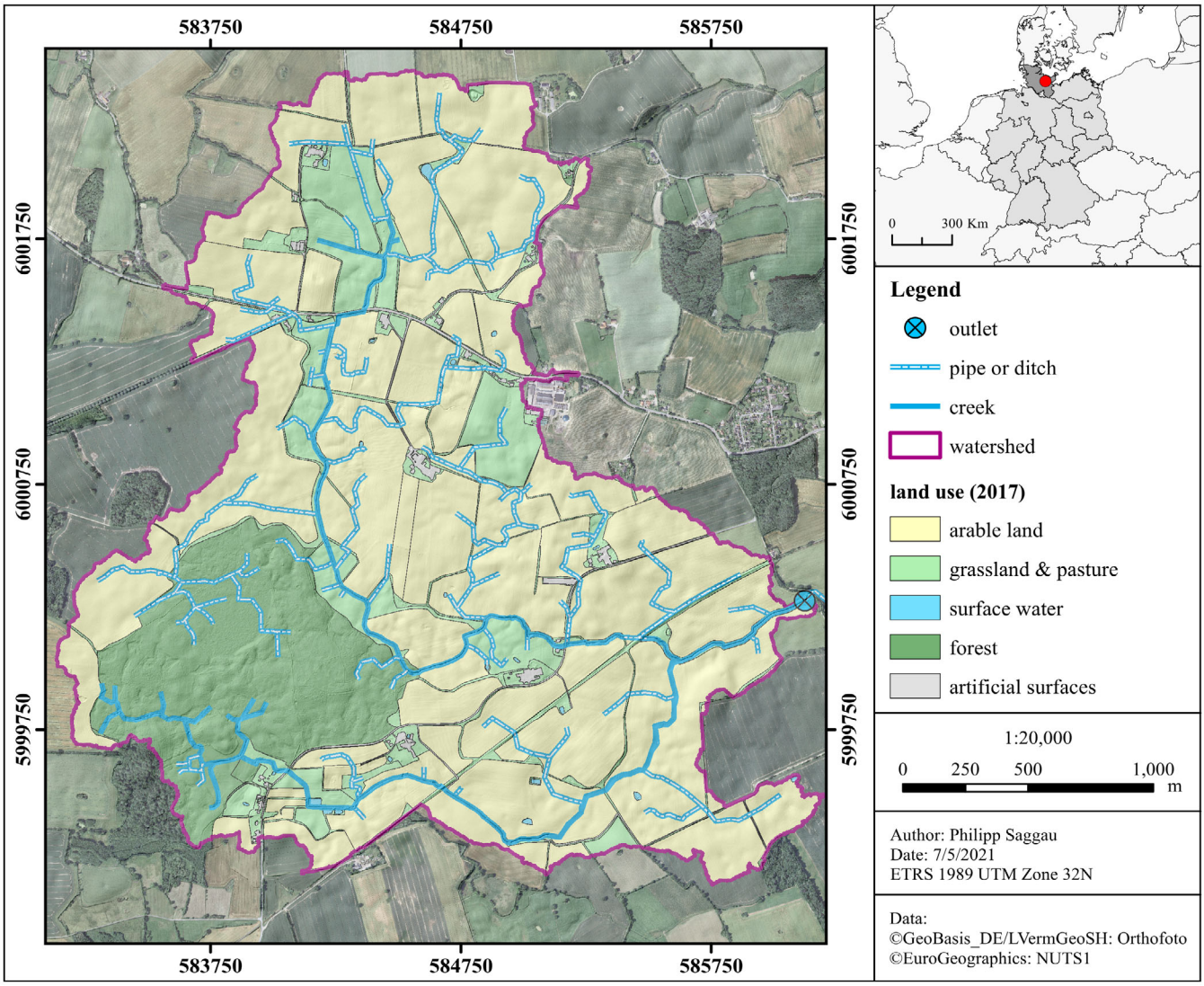

FIGURE 2 Land use and drainage network of the study area [Colour figure can be viewed at wileyonlinelibrary.com]

2 | MATERIAL AND METHODS

2.1 | Study area

The study was conducted in the Eastern Uplands of Schleswig-Holstein (Northern Germany, Figure 2), an area formed by glacial deposits of the Weichselian Glaciation (54°13′–54°16′ N, 10°27′–10°32′ E) (Figure 2). The study area comprises a 5.7 km^2 catchment of the Mühlenbach Creek, which is part of the Schwentine River basin. The catchment is characterized by a complex hummocky topography and widely occurring undrained depressions (kettle holes). Elevation of the site ranges between 35 and 63 m a.s.l. with an average slope of 5.5%. The climate is oceanic (Cfb) according to Köppen & Geiger (Peel et al., 2007) with mean annual temperature of 8.1°C and precipitation of 721 mm (weather station Doernick, DWD). Parent material is glacial till, which predominantly formed Luvisols (IUSS Working Group WRB, 2015) with loamy soil textures. Soils of steep slopes are frequently degraded and dominated by Regosols with coarser textures, while foot slopes are often covered by fine-textured colluvial deposits (Fleige & Horn, 2000). About 70% of the catchment is arable land, crossed by a complex network of artificial drainages and ditches. The dominant crop rotation is winter wheat (*Triticum aestivum* L.), winter barley (*Hordeum vulgare* L.) and winter rape (*Brassica napus* L.).

2.2 | Soil sampling and laboratory analysis

Disturbed soil samples were taken from 350 points based on randomized stratified sampling. Soil sampling was conducted in autumn 2017 and 2018. Samples were taken from a depth of 0–30 cm. Positions of the sampling sites were recorded by an RTK-dGPS (Leica Viva CS 10, GNSS GS08 plus).

Soil samples were air-dried (35°C) and sieved to <2 mm for further analyses. Total carbon content was determined by dry

combustion using a CN elemental analyzer (EURO EA HEKAtech). Carbonate content was determined by Scheibler analysis (Blume et al., 2010) and subtracted from total carbon for the derivation of soil organic carbon (SOC) content. Particle size distribution was analyzed by the combined sieve and sedimentation method (NAW, 2002). The subfractions of soil texture were classified according to the German classification standards. The degree of soil coverage was determined at each sampling site following the instructions of DVWK, 1996).

2.3 | Model design

2.3.1 | Model selection and description

For soil erosion modeling the process-based model E3D (version 3.3.0.132; Schmidt, 1991; Von Werner, 2007) has been selected for the following reasons:

1. the model is raster-based and fully distributed allowing the reduction of cell size for the implementation of tramlines;
2. E3D simulates surface runoff, sediment budgets, and sediment delivery to surface waters (Jetten et al., 2003; Starkloff & Stolte, 2014);
3. it has been extensively tested for Germany and has been applied in numerous studies, (e.g., Hänsel et al., 2018; Routschek et al., 2014; Schindewolf & Schmidt, 2012; Schmidt et al., 1999);
4. E3D offers a parameter catalog (Michael et al., 1996) for automated processing by derivation of soil parameters as a function of soil texture, land use, tillage, and simulation date. The parameter catalog is based on extensive data and is integrated in the software DPROC-version 1.9 (Von Werner, 2009; Schindewolf et al., 2013).
5. E3D showed promising results for parameterization of tramlines at the field-scale (Saggau et al., 2019).

Since E3D is described in detail by (Schmidt, 1991; Schmidt, 1992; Starkloff & Stolte, 2014), we briefly outline the main sub-processes simulated, which are: (i) infiltration of precipitation (Green & Ampt, 1911), (ii) discharge generation and detachment of soil particles using the momentum flux approach (Schmidt, 1991; Schmidt, 1996), (iii) transport and deposition of fine soil material. The latter depends on the transport capacity of overland flow and the concentration of soil particles along the transport path (Hänsel et al., 2018; Von Werner, 2007), considering the grain size distribution of the transported sediment and the sediment delivered to downstream water courses (Routschek et al., 2014).

Furthermore, the application of E3D requires site-specific information: (i) relief data [elevation 9m], (ii) precipitation data (date, time, and intensity [mm]) and (iii) soil data that comprise eight soil parameters: particle size distribution (% mass), bulk density (BD; kg m^{-3}), soil organic carbon content (SOC; % weight), initial soil water content (SWC; % volume), erosional resistance (N m^{-2}), hydraulic surface roughness (s $m^{-1/3}$), soil cover (% area) and skin factor (−).

2.3.2 | General model parameterization

To assess the impact of tramlines on soil erosion, two parameterizations were simulated and subsequently compared; a tramline parameterization (TLP) and a common parameterization (CP) without tramlines (cf. Figure 3 and Section 2.3.4). Because the tramline area is dependent on tyre width, which typically ranges from 429 to 752 mm (ten Damme et al., 2019), the choice of an adequate cell size is essential. In this study we followed the suggestions of Saggau et al. (2019), recommending a raster cell size of 1 m for all datasets, which is a compromise between model accuracy and maximum processing cell size within E3D for the investigated catchment.

For soil erosion modelLing, a single rainstorm event from October 4th, 2017 was chosen. Freely available precipitation data (https://opendata.dwd.de/) with a temporal resolution of 5-min intervals from official weather station Doernick (German National Meteorological Service; DWD), located 2.5 km east of the study area, were used. The rainstorm considered in our study lasted 33 hr and 10 min amounted to a total precipitation of 61.02 mm and reached a maximum five-minute rainfall intensity of 1.55 mm.

The digital elevation model (DEM) was provided by the Governmental Surveying Office of the German Federal State of Schleswig-Holstein (LVermGeo, 2005–2007). Its spatial resolution is 1×1 m (horizontal accuracy ±30 cm; vertical accuracy ±20 cm). High-resolution DEMs need to be corrected prior to use in hydrodynamic models such as E3D in order to ensure surface hydrologic connectivity and accurate representation of overland surface flow (Poppenga & Worstell, 2016; Rieger, 1998; Walker et al., 2021). Therefore, we used a hydrologic enforcement method, by burning streams, culverts, and artificial drainage structures (e.g., tile drainages) into the DEM. Agricultural drainage structures were localized by our own surveys, local drainage plans, and information from local farmers. The hydrologically-corrected DEM was then filled using the procedure developed by Wang & Liu (2006). This approach made it possible to optimize hydrological conductivity by reducing the artificially filled area of the original DEM by 85.2% which accounts for 0.9% of the total cells. To calculate the minimum upstream area, which is needed to define a flow channel within E3D, the critical source area (CSA) was set to 35,000 raster cells (m^2). This value was found to provide the best (visual) representation of the drainage system in the investigated catchment. For flow-routing, the FD8 algorithm was used within E3D.

Soil layers used as input for erosion modelling were constructed by spatial interpolation of SOC and the individual fractions of soil texture measured at 350 sampling points for the depth of 0–30 cm. For interpolation kriging with external drift (KED; McBratney et al., 2000; Hengl et al., 2003) was applied, using terrain attributes (e.g., topographic wetness index, slope) as auxiliary variables. For soil texture fractions, compositional KED was used. The resulting soil raster layers were integrated in E3D. The performance of the predicted soil variables is shown in Table 1. A detailed documentation of the interpolation procedure is available via Zenodo (https://doi.org/10.5281/zenodo.5153427).

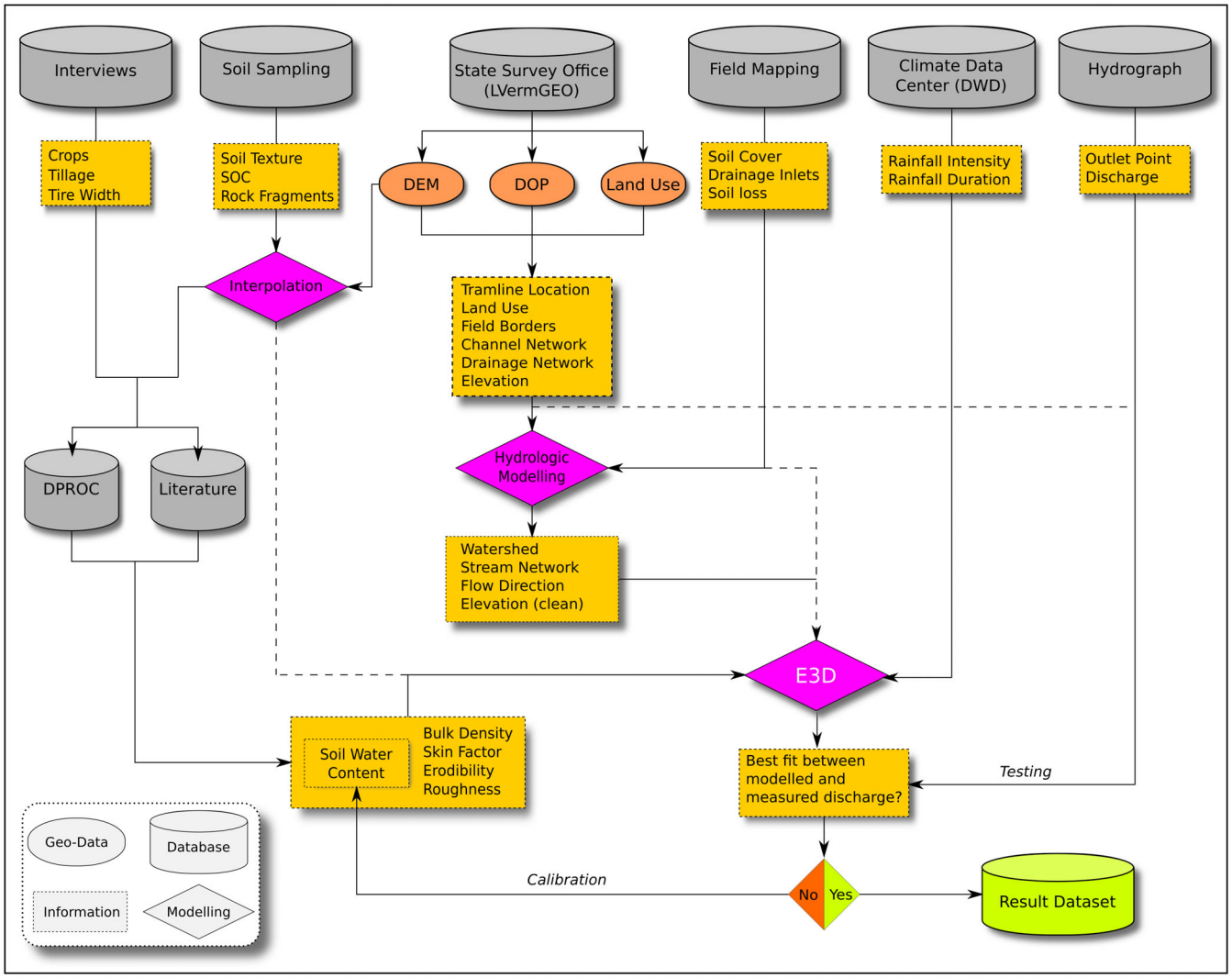

FIGURE 3 Scheme of the modelling approach. Input data handling, parameterization, calibration and modelling (DEM, digital elevation model; DOP, digital orthophoto; E3D, EROSION 3D; DPROC, data-base processor for E3D) [Colour figure can be viewed at wileyonlinelibrary.com]

	Sand			Silt				
Method	**Coarse**	**Medium**	**Fine**	**Coarse**	**Medium**	**Fine**	**Clay**	**SOC**
RMSE	3.67	4.85	5.27	2.94	2.07	1.69	3.69	1.31
MAE	2.04	3.45	3.85	2.15	1.49	1.20	2.69	0.71
R^2	77.6	37.2	66.3	18.8	40.9	32.7	41.5	0.8

TABLE 1 Model performance of kriging with external drift (KED) for the seven considered soil texture fractions (compositional) and soil organic carbon content (SOC) by means of root mean square error (RMSE), mean absolute error (MAE) and coefficient of determination (R^2) based on leave-one-out cross validation (LOOCV)

The degree of soil coverage for every individual field was derived from aerial photographs (RGB-camera) using a supervised classification (maximum-Likelihood) in ENNVI-version 5.4 (L3Harris Geospatial). To optimize the calculation of infiltration rates in E3D, rock fragment content (% mass) from soil sampling was included in the model. The soil parameters SWC, hydraulic surface roughness, erosional resistance, and skin factor were taken from DPROC. Management information about tillage practice and cultivated crop type were obtained from detailed interviews with local landowners and farmers.

2.3.3 | Parameterization of tramlines

The courses and widths of tramlines were derived from digital orthophotos (LVermGeo, 2017), with a ground resolution of

20 × 20 cm taken in the crop period of the investigated soil erosion event. Rasterization of tramline areas was performed for the outer width of the wheel tracks as shown in Figure 4. According to the raster-based generalization, the mean areal share of tramlines is about 13.5% per arable field. This accounts for 50.4 ha (8.8%) of the total catchment, which is an increase of about 76% compared to the real tramline extent (7.7% per arable field).

For each corresponding tramline raster cell, values for erosional resistance and hydraulic surface roughness were derived from the parameter catalog, which also provides a selection of estimates for tramlines. Soil cover values for tramlines were adapted by excluding vegetation cover from the total soil cover. The BD values suggested by DPROC (for unwheeled areas) were increased by 15% for tramline-cells based on Fleige & Horn (2000), who recorded mean bulk densities of about 1.4 g·cm^{-3} for the topsoil of cultivated fields and 1.6 g·cm^{-3} for tramlines based on comparative measurements of similar soils at the same times within a year. To account for the micromorphology of tramline ruts, we reduced the elevation in the DEM for tramline-cells by 5 cm, following the average tramline wheeling depths measured by Fleige & Horn (2000).

2.3.4 | Calibration and model testing

In our study, E3D was calibrated against total discharge, measured by a gauging station equipped with a portable sampling system (ISCO 6172) at the catchment outlet. The recording interval was set to 1 min. For calibration, SWC was adapted due to its high sensitivity in E3D and extended artificial drainage networks within the catchment. The best fit between modelled and measured discharge was achieved by reducing SWC by 20% (Figure 5). This setting was subsequently applied for all further model applications. In total, the reduced SWC

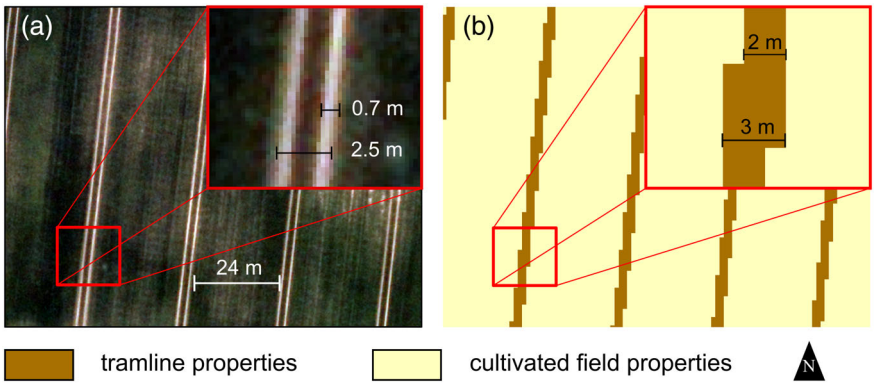

FIGURE 4 Generalization of (a) original tramlines from orthophotography into (b) rasterized tramlines for tramline parameterization (TLP) based on 1 × 1 m resolution [Colour figure can be viewed at wileyonlinelibrary.com]

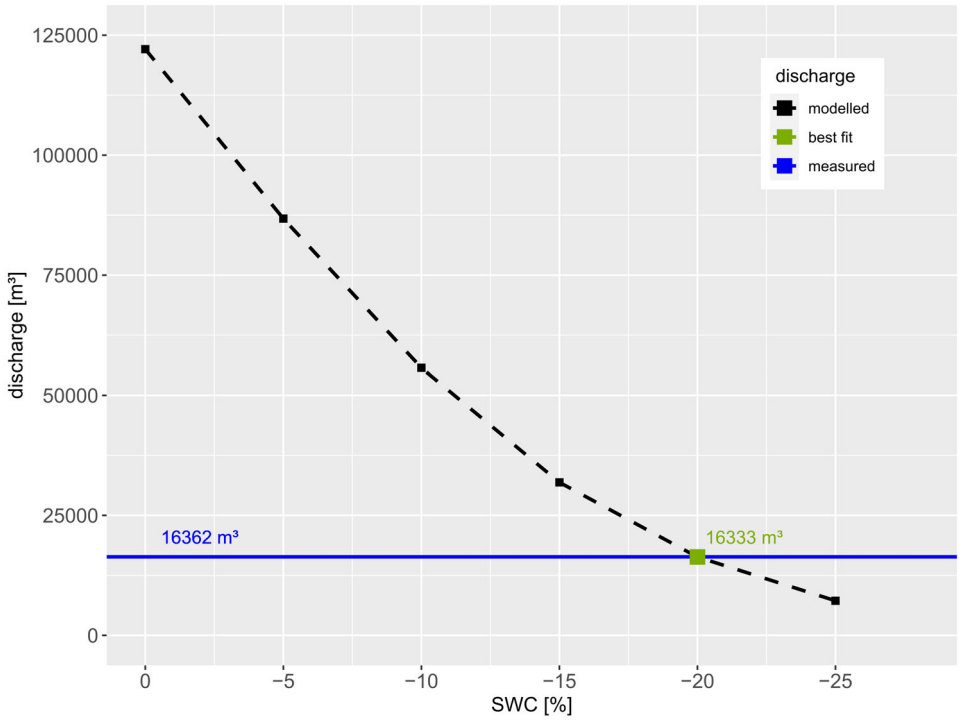

FIGURE 5 Model calibration of EROSION 3D (E3D) for tramline parametrization (TLP) based on the dependence between volumetric initial soil water content (SWC) and measured discharge [Colour figure can be viewed at wileyonlinelibrary.com]

led to a mean absolute decrease of about 5.8% compared to the suggested SWC of DPROC. The estimated total discharge of the calibrated TLP is about 0.17% lower than the measured.

For testing the modelled negative sediment budget against real numbers of eroded soil masses, soil erosion mapping was conducted, directly after the rainfall event on 28 fields within the catchment based on the instructions given by DVWK (1996). Soil loss was estimated by measuring the length and cross-sectional area of linear erosion features (e.g., rills) (e.g., Ledermann et al., 2010) with RTK-dGPS. To calculate the masses of eroded soil from soil volume estimates, the latter were multiplied with BD data taken from the E3D input layer used for TLP. Sheet erosion was documented but not included for soil loss calculations, because it cannot be quantified by exact measurement.

2.4 | Statistical analysis and reproducibility

To evaluate the importance of individual tramline properties on soil erosion, a nominal range sensitivity analysis (Cullen & Frey, 1999; Frey & Patil, 2002) was conducted. Here, we changed one of the adapted tramline parameters of TLP at a time by using all others from CP. Afterward, the implications of each model run on the modelling outcomes (e.g., soil erosion, runoff) were compared.

For statistical analysis of the dependent model variables, soil erosion and runoff, among tramlines, cultivated areas, and total fields unpaired two-samples Wilcoxon-tests were applied to evaluate differences. The $p < 0.05$ level was considered to be significant.

All statistical analyses, pre- and post-processing routines were progressed in R-version 1.4.1106 (R Core Team, 2021) and QGIS-version 3.4.7 (QGIS.org, 2021). For reproducibility, raw data and programming codes used in this study are documented and accessible via ZENODO (https://doi.org/10.5281/zenodo.5153427).

3 | RESULTS

3.1 | Model results of tramline (TLP) and common parameterization (CP)

The integration of tramlines in E3D revealed that 172.8 ha of the catchment (30.3%) is affected by soil erosion processes (53.3% erosion; 46.7% deposition). Compared to CP, it causes a slight increase of the area affected by erosion of 1.7 ha (+1.9%) while sediment deposits cover an additional area of about 18.5 ha (+30%) inside the catchment. Accordingly, the calculated sediment budget points to a more diverse distribution of erosion and deposition patterns for TLP. Field 1000 (Figure 6) shows how accumulation rates and areas are increased at sites where tramline erosion dominates. Cells with high deposition are common at foot slopes and concave terrain surfaces, like depressions, and are frequently found on the sides of tramlines.

Related to the total catchment, TLP indicates an average soil loss of 17.0 ± 230.8 Mg ha^{-1}. This equals a total of 9738.7 Mg of relocated and redistributed soil, which is 2.1-times higher than the amount calculated for CP. Moreover, soil loss calculated for TLP mainly occurs on arable fields (99.7%), but reveals a high variation in runoff and soil erosion, especially along the tramlines (Table 2).

TLP shows that soil loss rates for tramlines are 13.2-times higher compared to the same sections of CP. This suggests that an area percentage of 8.8% covered solely by tramlines, contributes to 71.9% of the total soil loss in the catchment. For TLP, the average runoff inside the tramline area reveals a mean of 1.4 ± 13.2 m^3m^{-1}, which is 2.3-times higher than that calculated for the cultivated land (0.6 ± 10.9 $m^3 \cdot m^{-1}$). The predicted increase in both soil loss ($p < 0.0001$) and runoff ($p < 0.01$) inside the tramlines is highly significant compared to the cultivated field area.

The comparison of runoff and soil loss, calculated for selected fields, according to TLP and CP, reveals a significant increase of both the simulated runoff volume and the amount of eroded soil in tramlines ($p < 0.0001$) as for the total fields (soil erosion, $p < 0.01$; runoff $p < 0.05$; Figure 7). Surprisingly, cultivated field areas show slightly higher soil loss in CP, although the increase in average runoff generation is 20% higher in TLP.

The mean soil loss rate of all arable fields in the catchment and the sediment delivery to channel arms considering all upstream subcatchments (Figure 8), indicates a strong increase of soil loss rate for most fields, which led to a change from 10.3 (±21.3) to 25.6 (±37.9) Mg per arable field (+148.5%). This increase of soil erosion for TLP promoted the increase of sediment input into the channel network by 61.2%, resulting in an additional amount of 7.9 Mg/ha^{-1} sediment entering the channel system of the catchment. The arms adjacent to fields with a higher soil loss rate are highly affected by an increased gain of sediment.

As shown in Figure 9, E3D calculated a total sediment delivery to the channel system of 4475.1 Mg for TLP which equals 45.9% of the total soil mobilized in the catchment. This equals an increase of 59.6% of soil (2803.3 Mg) and 41.4% of runoff delivery to channel network compared to CP. In addition, TLP shows differences in the predicted proportion of sediment particle sizes delivered to watercourses. Finally, clay and silt fractions increase by 5.5% (in total 32.7%) and 7.9% (in total 60.8%) at the expense of the sand proportion.

3.2 | Sensitivity analysis of tramline parameters

Figure 10 shows that the adopted BD values in tramlines cause the strongest increase in soil loss rates (+33%) and runoff (+27.9%) compared to CP, which also resulted in the highest increase in sediment input to surface waters (+32%). Erosional resistance of tramlines is estimated to affect average soil loss with a gain of 9.8% and an additional sediment delivery of 8.6% to channels. In general, erosional resistance, defined by particle and aggregate size and stability (Schmidt, 1991), specifically affected the composition of mobilized soil particle fractions, with higher proportions of silt and clay. Hydraulic surface roughness and soil cover in tramlines were discovered to have no stronger impact on soil erosion (+ < 1%) and even less for runoff

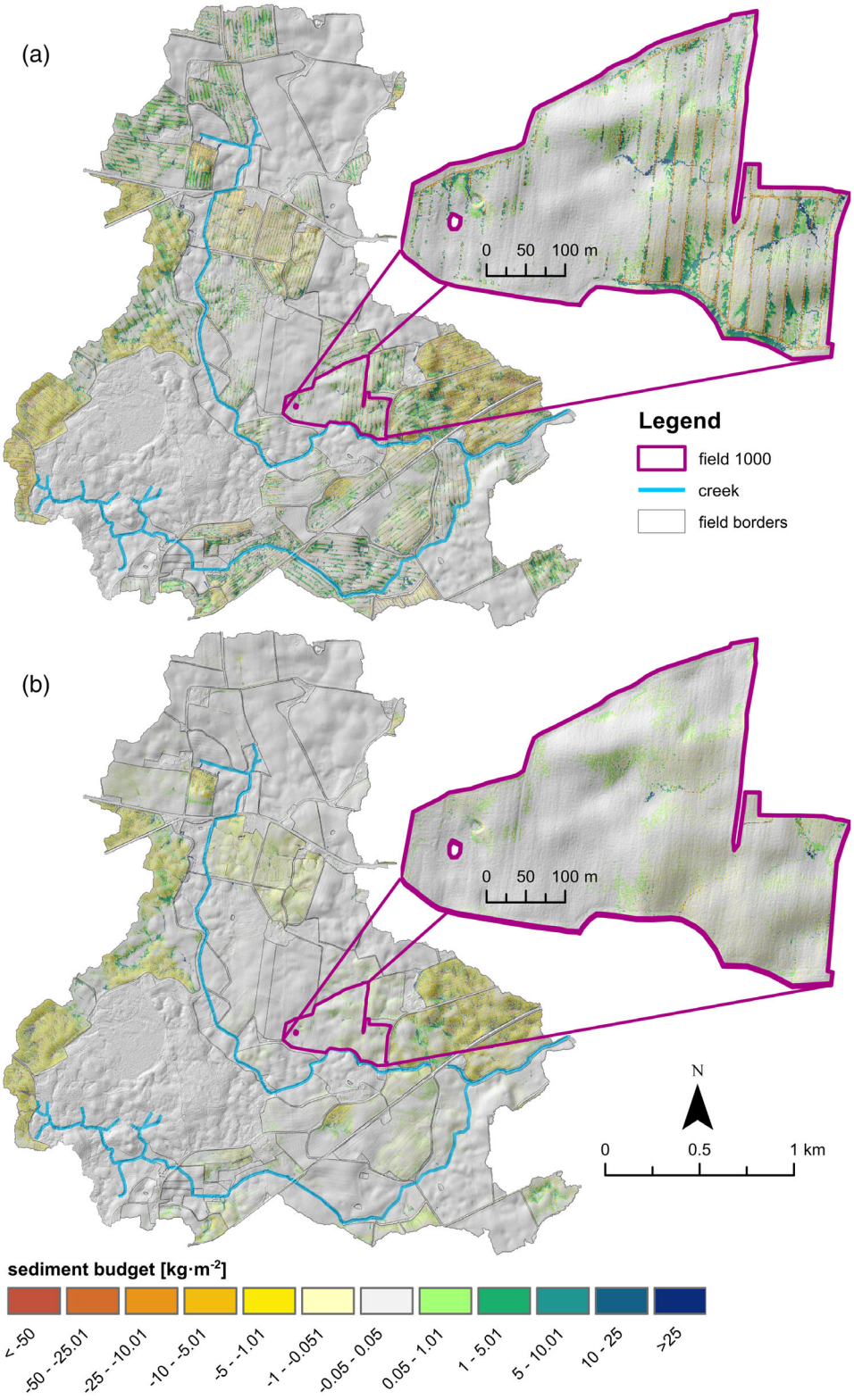

FIGURE 6 Predicted sediment budget of the catchment by E3D for (a) tramline parameterization (TLP) and (b) common parameterization (CP) with additional focus on one selected field (field 1000) [Colour figure can be viewed at wileyonlinelibrary.com]

(+ < 0.1%). The integration of tramline ruts in the DEM showed the second highest increase in average runoff of about +3%, while its effect in soil loss was low (+0.4%). Surprisingly, total sediment delivery to the channels was even reduced by - 0.2% (4.9 Mg) for adapted micro-morphology compared to CP.

3.3 | Testing of modeled soil loss

Soil erosion mapping showed measurable linear soil loss on four of 28 fields (Figure 11). All other fields showed clear evidence of severe interrill erosion in nearly all tramline areas as well as in

TABLE 2 Model predictions of EROSION 3D (E3D) for soil erosion and runoff based on the tramline parameterization (TLP) and the common parameterization (CP), separated by different field zones

Model output	Model input	Field zone	Area (km^2)	Mean	SD (±)	Min	Max	Med	Sum
Soil Erosion (Mg ha^{-2})	TLP	Tramlines	0.5	138.9	626.9	0.0	95,784.3	0.0	6999.7
		Cultivated	3.2	8.4	174.0	0.0	86,995.9	0.0	2708.7
		Non-Arable	2.0	0.2	16.6	0.0	10,740.3	0.0	30.3
		Catchment	5.7	17.0	230.8	0.0	95,784.3	0.0	9738.7
	CP	Tramlines	0.5	10.5	295.7	0.0	59,573.4	0.0	531.1
		Cultivated	3.2	13.2	351.4	0.0	99,786.6	0.0	4252.0
		Non-Arable	2.0	0.2	22.5	0.0	16,696.4	0.0	40.3
		Catchment	5.7	8.4	278.4	0.0	99,786.6	0.0	4823.4
Runoff (m^3 m^{-1})	TLP	Tramlines	0.5	1.4	13.2	0.0	1278.5	0.1	723,412.2
		Cultivated	3.2	0.6	10.9	0.0	1348.3	0.0	2,021,622.8
		Non-Arable	2.0	0.4	9.5	0.0	693.1	0.0	889,332.0
		Catchment	5.7	0.6	10.7	0.0	1348.3	0.0	3,634,366.9
	CP	Tramlines	0.5	0.4	6.4	0.0	956.6	0.0	190,159.2
		Cultivated	3.2	0.5	8.9	0.0	1147.4	0.0	1,629,511.2
		Non-Arable	2.0	0.4	8.4	0.0	569.0	0.0	792,460.8
		Catchment	5.7	0.5	8.5	0.0	1147.4	0.0	2,612,131.1

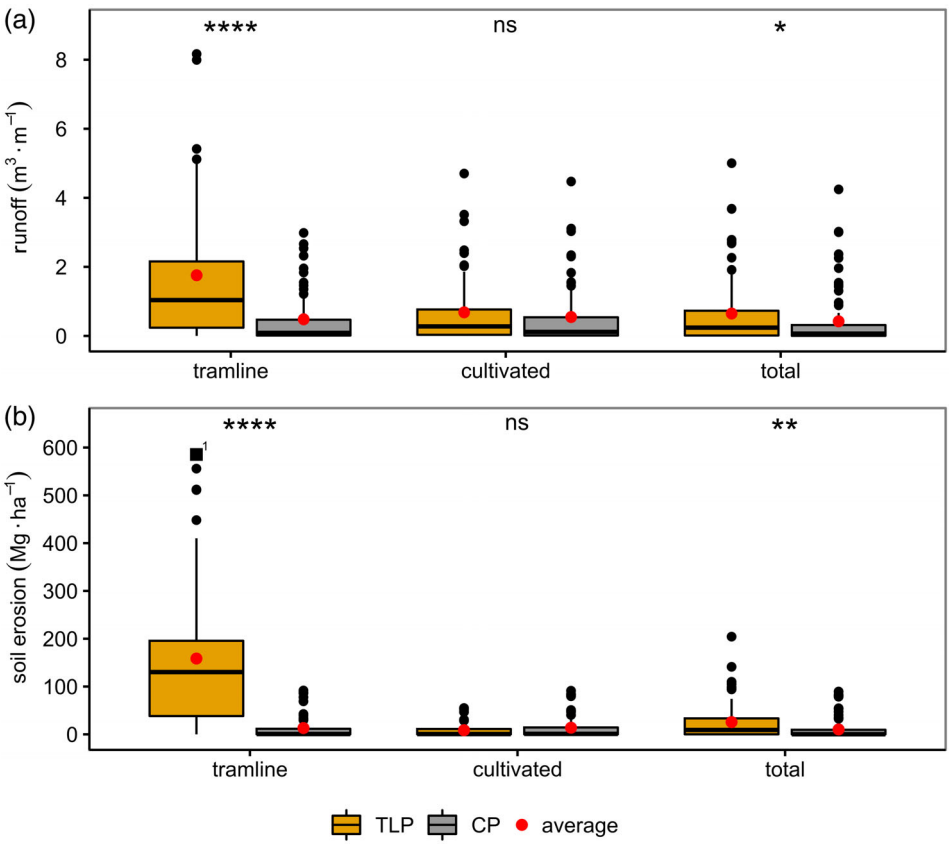

FIGURE 7 Box plots of results for (a) average runoff and (b) average soil loss rates based on arable fields (N = 75), comparing tramline area, cultivated area outside the tramlines and the entire field (total) by applying the tramline parameterization (TLP; orange) and the common parameterization (CP; gray). Significance levels: Ns: $p > 0.05$, *: $p <= 0.05$, **: $p <= 0.01$, ***: $p <= 0.001$ ****: $p <= 0.0001$. ■^{1}: further outliers: 595.7, 750.4, 1370.0 [Colour figure can be viewed at wileyonlinelibrary.com]

concave slope features, which were regularly accompanied by colluvial deposits in depressions. For the four fields with dominating linear erosion (Table 2), we registered 96 rills with a maximum length of 119.8 m (average 32.8 m) and a total soil loss of 53.9 Mg.

The spatial distribution of modeled erosion and deposition within the catchment corresponds qualitatively well to our field observations. It was also found that the predicted transfer points for sediment input into the river network fit accurately to the mapped locations. Modelled soil loss rates for TLP are higher for each mapped field and field

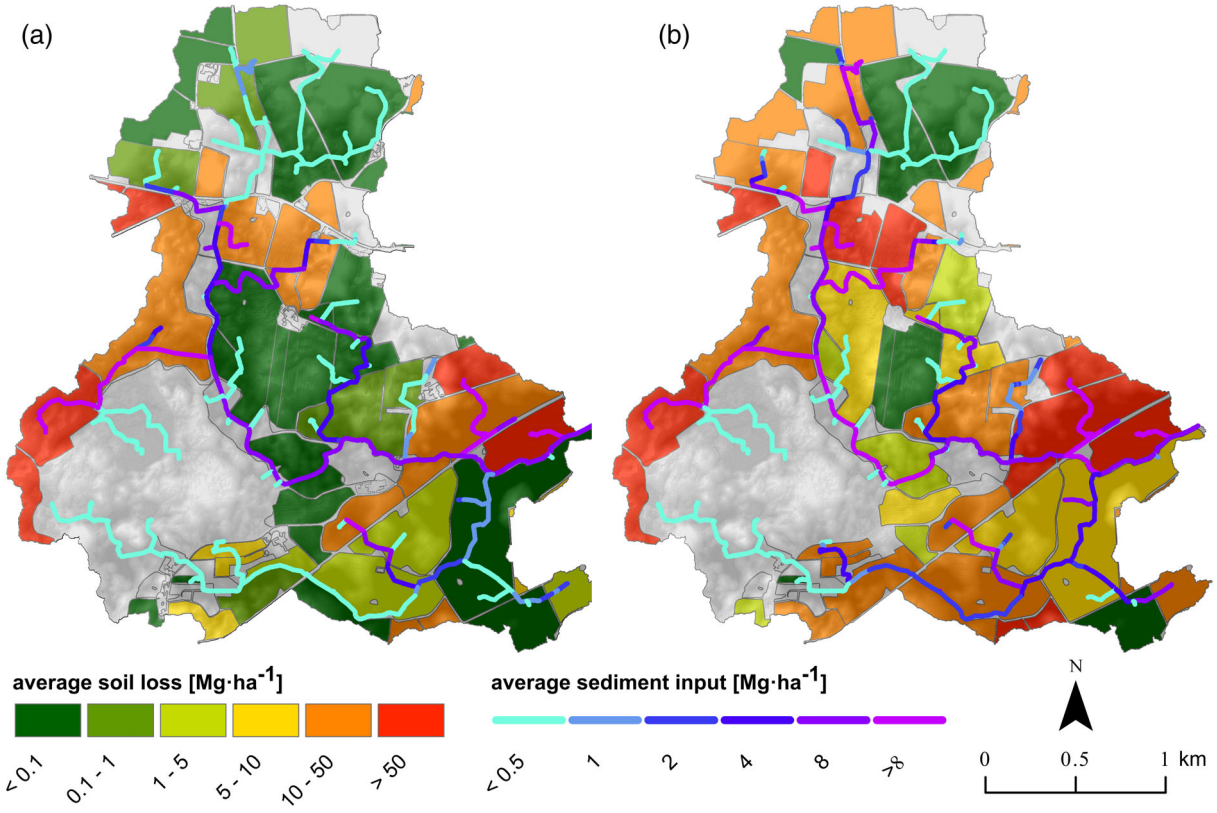

FIGURE 8 Simulated average soil erosion rates on arable fields and average sediment delivery to channel arms of the up lying watershed based on (a) the common parameterization (CP) and (b) the tramline parameterization (TLP) [Colour figure can be viewed at wileyonlinelibrary.com]

FIGURE 9 Predicted sediment delivery to channel network (a) and total channel flow (b), by comparing common parameterization (CP) and tramline parameterization (TLP) [Colour figure can be viewed at wileyonlinelibrary.com]

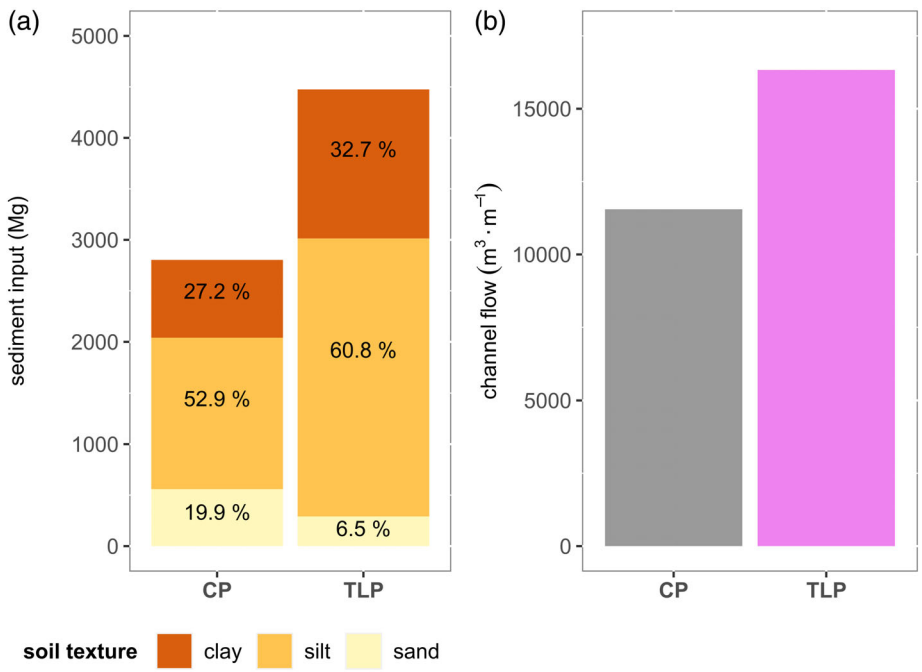

section, which range from the same magnitude to two orders of magnitude above the measured soil loss. However, soil loss rates for tramlines were highest in both the modeling results and the estimates derived from mapping. E3D predicted maximum soil loss rates in tramlines of field 1001 (346.5 Mg ha^{-1}), which was also the highest soil loss rate from measurements (7.2 Mg ha^{-1}).

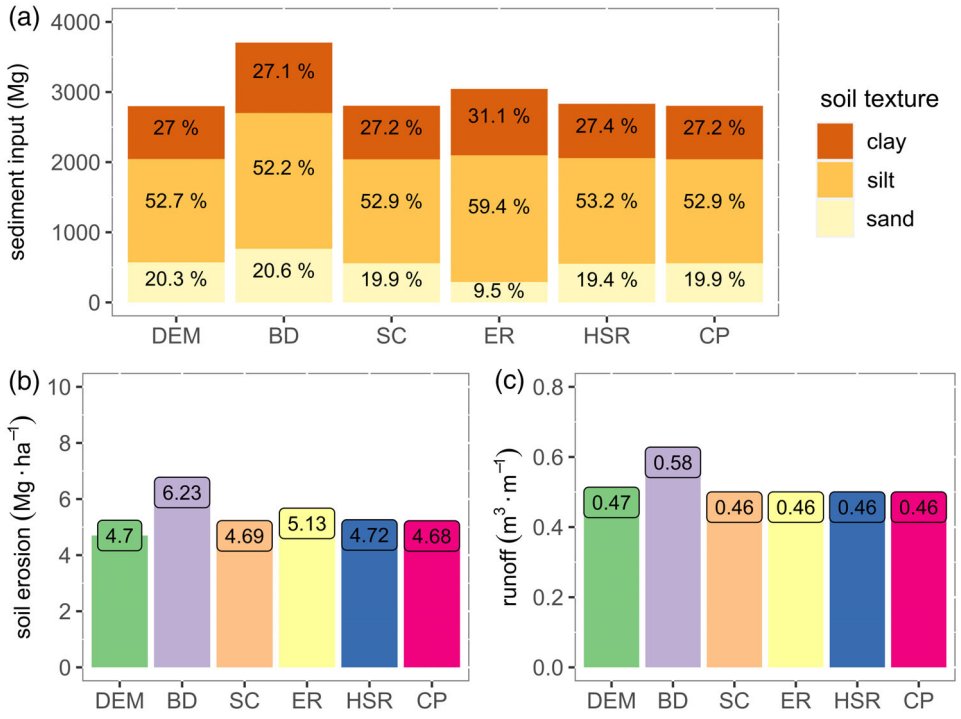

FIGURE 10 Sensitivity of adapted tramline parameters in E3D (DEM, digital elevation model; BD, bulk density; SC, soil cover; ER, erosion resistance; HSR, hydraulic surface roughness; and CP, common parameterization) for (a) sediment input and particle distribution to channel system, (b) average soil loss (c) and average runoff, based on the total catchment [Colour figure can be viewed at wileyonlinelibrary.com]

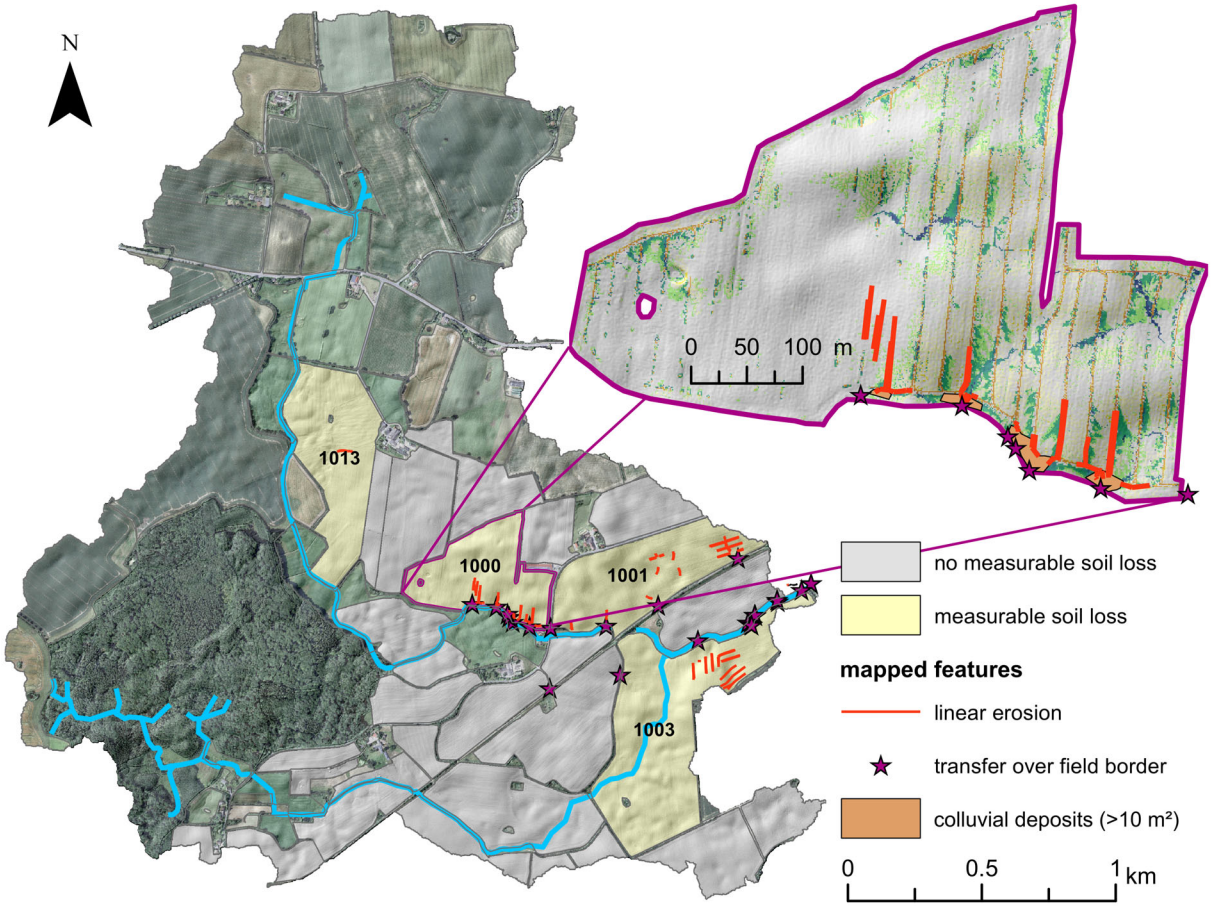

FIGURE 11 Spatial location of mapped soil erosion features for investigated fields during the mapping campaign with additional focus on one selected field (field 1000) [Colour figure can be viewed at wileyonlinelibrary.com]

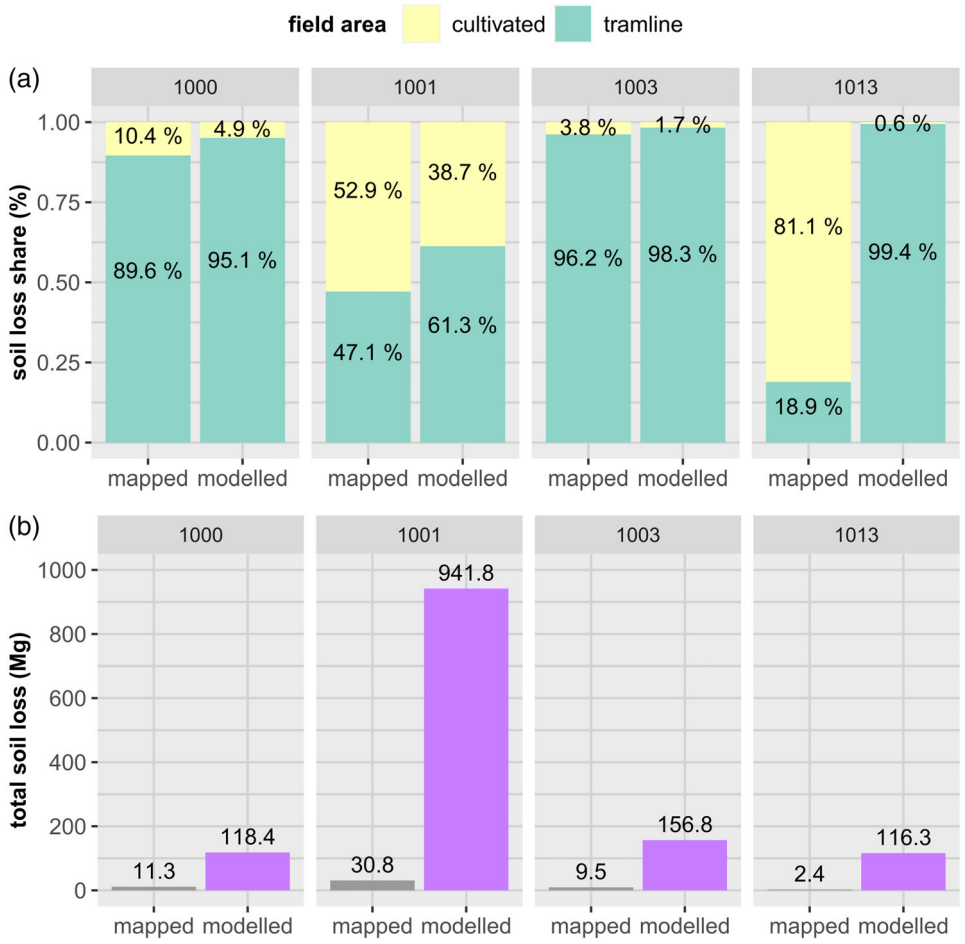

FIGURE 12 Comparison of model results from the tramline parameterization (TLP) with soil erosion mapping for four comparable fields (field 1000, 1001, 1003, 1013), considering (a) soil loss share from tramlines and cultivated areas and (b) total soil loss amounts [Colour figure can be viewed at wileyonlinelibrary.com]

The shares of absolute soil loss between tramlines and cultivated area for mapped and modeled results of TLP (Figure 12) show, that except for field 1013, the proportion of soil loss in the other fields is in good agreement between modelled and measured soil erosion (± 1.9%–14.2%). The figure also shows that predicted soil loss for the tramlines share is overestimated in all fields. In case of fields 1000 and 1003, soil erosion in tramlines dominates for measured and modelled estimations, while field 1001 reveals higher proportions of soil loss for cultivated areas. For field 1013, the proportions of modelled and mapped erosion do not match. In this case, E3D predicted soil loss almost exclusively from tramlines, while 81.1% of measured rill erosion was located in cultivated areas. Considering the total mass of soil moved within the fields, modelled soil loss is one (1000 and 1001) to two (1003 and 1013) orders of magnitudes higher. While the highest (field 1001) and lowest (field 1013) soil losses fit the predicted estimates, modeled soil loss for field 1000 was comparably low despite high measured estimates.

4 | DISCUSSION

4.1 | Indications from model results

Our results highlight that tramlines integrated into process-based models can significantly contribute to runoff and soil loss calculations in a catchment, resulting in a more realistic prediction of soil erosion risk. The estimated addition of tramlines to runoff (2.3 times) is in good agreement with Fleige & Horn (2000) who found an increase in runoff by a factor of 4 on similar soils. The integration of tramline ruts in the DEM results in a significant improvement in runoff prediction, and seems to be a key mechanism in the adequate parameterization of tramlines for process-based models.

According to the sensitivity analysis, the increases in runoff and soil loss inside the tramlines are mainly attributed to the process of soil compaction, rather than the lack of vegetation cover. Compaction through repetitive wheeling successively reduces micro-morphology, surface roughness, soil erosion resistance, and increases BD (Batey, 2009; Mosimann et al., 2008; Weisskopf et al., 2010). The latter was found to be the key parameter responsible for increases in soil loss and runoff, as reported by others (Govers et al., 1990; Hieke & Schmidt, 2013; Parker et al., 1995). Under the given conditions the degree of soil coverage from vegetation was identified as an insensitive parameter that contributes only a little to changes in modelled soil erosion rates. This apparent contradiction certainly results from the fact that the rainfall event investigated in this study occurred at an early stage of crop development. Consequently, vegetation cover is expected to play a more vital role with progressing phenological cycle of the crops. Thus, soil compaction is the main process responsible for soil erosion processes in tramlines, but its dominance may shift depending on the time of the year.

Interestingly, mobilized soil fractions of silt and clay increased within tramlines due to reduced erosional resistance, which is dependent on, for example, aggregate size and stability (Schmidt, 1991). This is in agreement with studies highlighting that soils with reduced aggregate size and stability (e.g., by compaction) release finer soil fragments (Leguédois & Le Bissonnais, 2004; Shi et al., 2017). As the proportion of mobilized finer fractions (silt and clay) preferentially bound nutrients such as P (Davison et al., 2008), it can be expected that tramlines are more affected by nutrient losses, which is supported by studies from Withers et al. (2006) and Silgram et al. (2010). Therefore, it can be concluded that tramlines not only increase soil erosion, but also the transport of nutrients, which are likely to cause environmental problems in adjacent ecosystems.

The unanticipated finding that runoff and soil erosion was increased but sediment input to channels reduced, suggests that tramline ruts influence water and sediment connectivity by channeling and redirecting runoff. In this case, the arrangement of tramlines in the catchment seems to have a slightly positive effect on sediment delivery by reducing overland flow connectivity.

The unanticipated lower soil loss on cultivated areas for TLP, compared to CP, could be explained by an intensified deposition. When runoff with an increased load of suspended sediment leaves the tramline, soil conditions, and relief of the cultivated field (e.g., hydraulic surface roughness and surface cover) reduce concentration and speed of overland flow, which consequently decreases its transport capacities. This favours deposition of soil particles, despite additions of runoff, as an increase in depositional areas consequently reduces the average and total soil loss within the cultivated fields for TLP.

Considering the implication of soil erosion for the investigated catchment, the estimated soil loss rates of our event exceeded the estimated annual average of soil loss for arable land in Germany (3.6 t ha^{-1} yr^{-1}; Saggau et al., 2017). Although the event in 2017 was the most erosive one within the period of 2016 and 2020, it shows that, in consideration of soil production rates (ca. 0.036 ± 0.04 mm yr^{-1}) (Montgomery, 2007) soil erosion, especially from tramlines, can be a major degradational process in Weichselian moraine landscapes affecting sustainable land management.

4.2 | Model performance

Soil loss prediction of TLP showed plausible and promising results when compared with the measured patterns and quantities of erosion (Section 3.3). Especially the good agreement of the share of modeled and measured amounts of soil loss from tramline and cultivated areas are promising (field 1000, 1001, 1003). The discrepancy between modeled and measured values for field 1013 can be explained by the fact, that in 2016 the field was divided into two smaller parcels. In this year the headland was located at the same spot where the rill system was found. Headlands are highly affected by compaction due to increased field traffic intensity (Augustin et al., 2020; Kuhwald et al., 2016) and thus may have favoured rill formation in 2017. This is in agreement with several studies (e.g., Prasuhn, 2020; Remund et al., 2021; Steinhoff-Knopp & Burkhard, 2018), who identified headlands as highly erosion prone areas, related to tramlines, which seems to be important determinants for soil erosion modeling.

The reason for the higher estimations supplied by E3D, compared to testing data, can be linked to the fact that the conducted resolution of 1x1 m, which was limited by the software and catchment-extent, resulted in an over-prediction of tramline area by 76%. This not only leads to an increase in erosion prone tramline area, but also to a combination of two small wheel tracks to one larger pathway with combined surface runoff. This generalization is likely to overestimate the severity of predicted runoff and soil erosion processes.

Furthermore, measured soil loss is only based on rill erosion and does not account for interrill erosion (e.g., sheet wash and raindrop splash). The share of interrill erosion from total erosion can, however, range from 10%–99% (Auerswald & Kainz, 1998; Bug & Mosimann, 2012; Govers & Poesen, 1988; Poesen et al., 2003). Interrill erosion is difficult to assess because of gaps in our knowledge regarding soil erosion processes (Poesen, 2018) and depends on several factors, for example, soil texture and climatic conditions (Evans et al., 2016). In Table 3 we integrated approximations for less pronounced interrill erosion (25%; Prasuhn, 2011) and dominant interrill erosion (75%; Bug, 2011). Suggesting a dominant interrill erosion of 75%, measured soil erosion rates are in the same or at least one order of magnitude lower and account for 16.2% of modeled soil loss. The calibration of E3D was a fundamental step, which improved model results noticeably, by narrowing runoff by 81.6% and soil erosion by 76.9% compared to uncalibrated modeling. Compared to other process-based studies, which report overestimations of two magnitudes (Jetten et al., 2003; Saggau et al., 2019; Schmidt et al., 1999; Starkloff & Stolte, 2014), our approach can be seen as a step forward in the optimization of model parameterization.

4.3 | Model uncertainties

Although the results point to an improvement in predicting soil erosion, some limitations remain that occur from variations and overestimations in the model outcomes (Section 3.3). These inaccuracies can be mainly addressed to deficits in the input data and model structure. The latter implies that process-based models such as E3D are to some extent based on empirical data from plot experiments. Plot-data incurs limitations for distributed modeling, as described by, for example, Batista et al. (2019), Parsons (2019), and Boardman & Evans (2020), thus those models are likely to overestimate severity and spatial extent of soil erosion.

In addition to the previously discussed overestimations of tramline area (Section 4.2), computational grid cell size is another important sensitive parameter that affects the outcome of grid-based modelling (Saggau et al., 2019). By changing spatial resolution, hydrological and geomorphological parameters (e.g., slope, slope length, catchment size) can vary considerably (Hancock & Evans, 2006; Jetten et al., 2003; Millares et al., 2012). Furthermore, model results also depend on the hydrologic preprocessing (e.g., flow-routing algorithm,

TABLE 3 Comparison of modeled soil erosion rates for tramline parameterization (TLP) and measured rill erosion rates based on fields with measurable soil loss subdivided into different field zones

		Soil loss rates (mg ha^{-1})			
Field ID	Field zone	Modelled	Measured rill erosion	25% interrill erosion	75% interrill erosion
1000	Cultivated	0.6	0.1	0.1	0.4
	Tramline	83.9	6.1	8.2	24.7
	Total	10.6	0.8	1.1	3.3
1001	Cultivated	28.6	1.0	1.4	4.2
	Tramline	346.5	7.1	9.5	28.6
	Total	65.4	1.7	2.3	7.0
1003	Cultivated	0.1	0.0	0.0	0.1
	Tramline	49.1	2.2	3.2	9.7
	Total	6.5	0.3	0.4	1.3
1013	Cultivated	0.1	0.1	0.2	0.5
	Tramline	49.1	0.2	0.2	0.6
	Total	7.7	0.1	0.2	0.5
Total	Cultivated	6.7	0.3	0.4	1.2
	Tramline	113.8	3.2	4.5	13.4
	Total	20.7	0.7	0.9	2.8

Note: For measured rill erosion rates, integrated shares of estimated 25% and 75% interrill erosion were added

CSA, hydro-enforcement method of the DEM), which affects flow direction, flow length, and slope characteristics (Poppenga & Worstell, 2016; Walker et al., 2021).

By including tile drains as part of the hydrologic system (Section 2.3), the spatial distribution of soil erosion processes is improved (Luetzenburg et al., 2020; Moloney et al., 2020). However, these pipes are treated as surface channels during the model routine, which allows runoff and sediment inputs at places where no direct surface connection is present. Therefore, sediment input and runoff gains in the channel system could be over-predicted in this study.

Other possible uncertainties rise from model calibration (Batista et al., 2019; Starkloff & Stolte, 2014), utilization of homogeneous rain data over the entire catchment, and by the input of soil-parameters derived by DPROC or literature (Sections 2.3.3 and 2.3.4). Accessible parameters for tramlines are especially rare and are likely to vary in space and time. As BD was shown to be a highly sensitive parameter within tramlines, it also has a high uncertainty potential. Furthermore, the importance of BD highlights that neglecting (compacted) headlands can negatively affect prediction accuracy.

4.4 | Future research needs

Our results highlight the need for more data on soil properties especially for tramlines. Specifically, the spatio-temporal variation of BD seems to be an important determinant. In general, the improvement of assessing accurate input data by offering error propagation is required in order to better understand the capabilities of model outcomes (Batista et al., 2019; Parsons, 2019). While we reviewed the uncertainties of certain input data (e.g., DEM, SOC, and soil texture), measures for other complex input-data (e.g., BD, erosional resistance, and hydraulic surface roughness) are still missing. The gap could be filled by utilizing geostatistical or machine learning approaches (e.g., Emadi et al., 2020; McBratney et al., 2003), or new measuring techniques using remote-sensing data (Martinez-Agirre et al., 2020). At the same time, data and scripts of such studies should be freely accessible in spirit of reproducibility, to facilitate exchange and progress in modelling (Kuhwald et al., 2020).

To further increase the spatial prediction accuracy in soil erosion modelling, the consideration of headlands seems necessary (Sections 3.2 and 4.1). Additionally, improvements in cell sizes below 1 × 1 m are expected to offer better results, with less over-prediction as it can more accurately account for tramline areas (Saggau et al., 2019). As soil erosion by water is a highly spatio-temporal process, which is predominantly driven by single events (Fiener et al., 2015; Wilken et al., 2018), continuous modelling over time is essential. Long-term simulations within a catchment should provide better and more meaningful results concerning the temporal role of tramlines on soil erosion and consequently soil degradation within an agricultural landscape.

Our study showed that water and sediment dynamics and connectivity within a catchment are strongly interrelated with tramlines. Consequently, their impact on water and sediment connectivity needs to be assessed, as connectivity is an important factor controlling soil erosion risk (Baartman et al., 2020; Boardman et al., 2019) and sediment delivery to channel networks (Section 4.1). In order to adapt

adequate measures for preventing soil degradation and establishing sustainable land management, our approach offers the possibility to evaluate the success of conservation measures concerning the reduction of soil loss related to tramlines e.g. direction to the slope, intermitting planting and tramline renovation (Damanauskas & Jablonskytė-Raščė, 2021; Mosimann et al., 2008; Withers et al., 2006). This was not possible until now, but needs to be evaluated, as soil erosion in tramlines seems to be a major process in agricultural soil degradation.

Finally, we showed that the impact of compacted tramlines on soil erosion and runoff can be severe. However, other landscapes with different environmental conditions and management practices might show a different response to tramlines. Accordingly, more studies in catchments with different environmental conditions are necessary to assess, where the risk of compacted tramlines is as serious as indicated in our study.

5 | CONCLUSIONS

We have demonstrated the application of a process-based soil erosion model that considers the effect of compacted tramlines for an entire catchment for the first time. The results highlight that:

1. Tramlines strongly influence sediment and runoff dynamics and increase sediment delivery to adjacent water systems.
2. Compaction induced increases of bulk density has the most severe impact on modeled soil loss and runoff generation in tramlines.
3. Tramlines are estimated to increase mobilized silt and clay proportions, which promotes the risk of P transport.
4. Adoption of tramline ruts in the DEM improves runoff prediction.
5. Model calibration strongly enhances model outcomes.

Despite general over-predictions and uncertainties of the model simulations, our results confirm that tramlines are serious sources of runoff and soil loss, which strongly increase sediment delivery to channel network. This study advances the application of process-based soil erosion models and demonstrates that compacted tramlines cannot be neglected when soil erosion and sediment delivery should be accurately assessed within a catchment. To adapt management practices to prevent soil degradation, our approach offers a way to implement tramline specific conservation measures into the model design and to assessing their effectiveness. This facilitates adequate implementation of soil erosion protection measures, which remains one of the most important goals in soil erosion modeling for the sustainable development of agricultural landscapes.

ACKNOWLEDGMENTS

First, we would like to give special thanks to the landowners and farmers of the study area, who freely provided sensible and valuable information for the study and made their lands accessible for investigation. Further the authors like to thank all students contributed to sampling and mapping. We thank M. van Werner for technical support with EROSION 3D and of course all our lab members for their contributions. We are grateful to James F. Petersen for linguistic editing. Finally, we thank A. Berger, M. Gosse, J. Goldmann, and V. Schroeren for comprehensive assistance in the lab analysis.

CONFLICT OF INTEREST

The authors declare no conflict of interest.

AUTHOR CONTRIBUTIONS

Conceptualization, Philipp Saggau and Michael Kuhwald; Data curation, Philipp Saggau and Michael Kuhwald; Investigation, Philipp Saggau; Methodology Philipp Saggau, Wolfgang Berengar Hamer and Michael Kuhwald; Software, Philipp Saggau and Wolfgang Berengar Hamer; Calibration and Validation, Philipp Saggau; Writing original draft, Philipp Saggau; Writing review & editing, Philipp Saggau, Michael Kuhwald, Wolfgang Berengar Hamer and Rainer Duttmann; Supervision, Rainer Duttmann

DATA AVAILABILITY STATEMENT

The distributable data that support the findings of this study are openly available in Zenodo at https://doi.org/10.5281/zenodo.5153427.

ORCID

Philipp Saggau https://orcid.org/0000-0002-4648-1650
Michael Kuhwald https://orcid.org/0000-0003-3346-2888
Wolfgang Berengar Hamer https://orcid.org/0000-0002-5943-5020

REFERENCES

Auerswald, K., & Kainz, M. (1998). Erosionsgefährdung (C-Faktor) durch Sonderkulturen. *Bodenschutz*, *3*, 98–102.

Augustin, K., Kuhwald, M., Brunotte, J., & Duttmann, R. (2020). Wheel load and wheel pass frequency as indicators for soil compaction risk: A four-year analysis of traffic intensity at field scale. *Geosciences*, *10*, 292. https://doi.org/10.3390/geosciences10080292

Baartman, J. E. M., Nunes, J. P., Masselink, R., Darboux, F., Bielders, C., Degré, A., Cantreul, V., Cerdan, O., Grangeon, T., Fiener, P., Wilken, F., Schindewolf, M., & Wainwright, J. (2020). What do models tell us about water and sediment connectivity? *Geomorphology*, *367*, 1–17. https://doi.org/10.1016/j.geomorph.2020.107300

Batey, T. (2009). Soil compaction and soil management - a review. *Soil Use and Management*, *25*, 335–345. https://doi.org/10.1111/j.1475-2743.2009.00236.x

Batista, P. V. G., Davies, J., Silva, M. L. N., & Quinton, J. N. (2019). On the evaluation of soil erosion models: Are we doing enough? *Earth-Science Reviews*, *197*, 1–17. https://doi.org/10.1016/j.earscirev.2019.102898

Blume, H.-P., Stahr, K., & Leinweber, P. (2010). *Bodenkundliches Praktikum: Eine Einführung in pedologisches arbeiten für Ökologen, insbesondere land- und forstwirte, und für geowissenschaftler, 3., neubearb. Aufl.* 3(1–255). Heidelberg: Spektrum Akademischer Verlag. https://doi.org/10.1007/978-3-8274-2733-5

Boardman, J., & Evans, R. (2020). The measurement, estimation and monitoring of soil erosion by runoff at the field scale: Challenges and possibilities with particular reference to Britain. *Progress in Physical Geography: Earth and Environment*, *44*, 31–49. https://doi.org/10.1177/0309133319861833

Boardman, J., & Poesen, J. (Eds.). (2006). *Soil erosion in Europe*. Chichester: Wiley.

Boardman, J., Vandaele, K., Evans, R., Foster, I. D. L., & Aitkenhead, M. (2019). Off-site impacts of soil erosion and runoff: Why connectivity is more important than erosion rates. *Soil Use and Management*, *35*, 245–256. https://doi.org/10.1111/sum.12496

Borrelli, P., Paustian, K., Panagos, P., Jones, A., Schütt, B., & Lugato, E. (2016). Effect of good agricultural and environmental conditions on erosion and soil organic carbon balance: A national case study. *Land Use Policy*, *50*, 408–421. https://doi.org/10.1016/j.landusepol.2015.09.033

Bug, J. (2011). *Modellierung der linearen Bodenerosion: Entwicklung und awendung von entscheidungsbasierten modellen zur flächenhaften prognose der linearen erosionsaktivität und des gewässeranschlusses von Ackerflächen (Niedersachsen und Nordwestschweiz)*. Dissertation. Inst. für Physische Geographie und Landschaftsökologie, Hannover: Leibniz-Universität.

Bug, J., & Mosimann, T. (2012). Lineare erosion in Niedersachsen – Ergebnisse einer elfjährigen messreihe zu ausmaß, kleinräumiger verbreitung und ursachen des bodenabtrags. *Die Bodenkultur*, *2-3*, 63–75.

Cullen, A. C., & Frey, H. C. (1999). *Probabilistic Techniques in Exposure Assessment*. New York: Plenum Press.

Damanauskas, V., & Jablonskytė-Raščė, D. (2021). New tillage system with additional renovation of soil properties in tramlines. *Applied Sciences*, *11*, 2795. https://doi.org/10.3390/app11062795

Davison, P. S., Withers, P. J. A., Lord, E. I., Betson, M. J., & Strömqvist, J. (2008). PSYCHIC – A process-based model of phosphorus and sediment mobilisation and delivery within agricultural catchments. Part 1: Model description and parameterisation. *Journal of Hydrology*, *350*, 290–302. https://doi.org/10.1016/j.jhydrol.2007.10.036

Deasy, C., Quinton, J. N., Silgram, M., Bailey, A. P., Jackson, B., & Stevens, C. J. (2009). Mitigation options for sediment and phosphorus loss from winter-sown arable crops. *Journal of Environmental Quality*, *38*, 2121–2130. https://doi.org/10.2134/jeq2009.0028

DVWK. (1996). *Bodenerosion durch Wasser. DVWK-Merkblatt 239: Kartieranleitung zur Erfassung aktueller Erosionsformen. [Soil erosion by water. DVWK-Bulletin 239: Mapping guideline for recording of actual erosion features]*. Bonn: Wirtschafts- und Verl.-Ges. Gas und Wasser.

Emadi, M., Taghizadeh-Mehrjardi, R., Cherati, A., Danesh, M., Mosavi, A., & Scholten, T. (2020). Predicting and mapping of soil organic carbon using machine learning algorithms in northern Iran. *Remote Sensing*, *12*, 1–34. https://doi.org/10.3390/rs12142234

Evans, R. (2017). Factors controlling soil erosion and runoff and their impacts in the upper Wissey catchment, Norfolk, England: A ten year monitoring programme. *Earth Surface Processes and Landforms*, *42*, 2266–2279. https://doi.org/10.1002/esp.4182

Evans, R., Collins, A. L., Foster, I. D. L., Rickson, R. J., Anthony, S. G., Brewer, T., Deeks, L., Newell-Price, J. P., Truckell, I. G., Zhang, Y., & Nicholson, F. (2016). Extent, frequency and rate of water erosion of arable land in Britain - benefits and challenges for modelling. *Soil Use and Management*, *32*, 149–161. https://doi.org/10.1111/sum.12210

Fiener, P., Auerswald, K., & van Oost, K. (2011). Spatio-temporal patterns in land use and management affecting surface runoff response of agricultural catchments—A review. *Earth-Science Reviews*, *106*, 92–104. https://doi.org/10.1016/j.earscirev.2011.01.004

Fiener, P., Dlugo, V., & Van Oost, K. (2015). Erosion-induced carbon redistribution, burial and mineralisation — Is the episodic nature of erosion processes important? *CATENA*, *133*, 282–292. https://doi.org/10.1016/j.catena.2015.05.027

Fleige, H., & Horn, R. (2000). Field experiments on the effect of soil compactionon soil properties, runoff, interflow and erosion. *Advances in GeoEcology*, *32*, 258–268.

Frey, H. C., & Patil, S. R. (2002). Identification and review of sensitivity analysis methods. *Risk Analysis*, *22*(3), 553–578. https://doi.org/10.1111/0272-4332.00039

Gillespie, G. D., & McDonnell, K. P. (2020). Estimating the current area of European tillage systems occupied by tramlines and a potential approach for the cultivation of this underutilised area. *Biosystems Engineering*, *197*, 1–11. https://doi.org/10.1016/j.biosystemseng.2020.06.004

Govers, G., Everaert, W., Poesen, J., Rauws, G., de Ploey, J., & Lautridou, J. P. (1990). A long flume study of the dynamic factors affecting the resistance of a loamy soil to concentrated flow erosion. *Earth Surface Processes and Landforms*, *15*, 313–328. https://doi.org/10.1002/esp.3290150403

Govers, G., Merckx, R., van Wesemael, B., & van Oost, K. (2017). Soil conservation in the 21st century: Why we need smart agricultural intensification. *The Soil*, *3*, 45–59. https://doi.org/10.5194/soil-3-45-2017

Govers, G., & Poesen, J. (1988). Assessment of the interrill and rill contributions to total soil loss from an upland field plot. *Geomorphology*, *1*, 343–354. https://doi.org/10.1016/0169-555X(88)90006-2

Green, W. H., & Ampt, G. A. (1911). Studies on soil physics. *The Journal of Agricultural Science*, *4*, 1–24. https://doi.org/10.1017/S0021859600001441

Hancock, G. R., & Evans, K. G. (2006). Channel head location and characteristics using digital elevation models. *Earth Surface Processes and Landforms*, *31*, 809–824. https://doi.org/10.1002/esp.1285

Hänsel, P., Kaiser, A., Buchholz, A., Böttcher, F., Langel, S., Schmidt, J., & Schindewolf, M. (2018). Mud flow reconstruction by means of physical erosion modeling, high-resolution radar-based precipitation data, and UAV monitoring. *Geosciences*, *8*, 1–21. https://doi.org/10.3390/geosciences8110427

Hengl, T., Heuvelink, G. B. M., & Stein, A. (2003). *Comparison of kriging with external drift and regression-kriging. Technical Note*. Enschede, The Netherlands: ITC. https://webapps.itc.utwente.nl/librarywww/papers_2003/misca/hengl_comparison.pdf

Hieke, F., & Schmidt, J. (2013). The effect of soil bulk density on rill erosion – Results of experimental studies. *Zeitschrift für Geomorphologie*, *57*, 245–266. https://doi.org/10.1127/0372-8854/2012/0091

IUSS Working Group WRB. (2015). *World reference base for soil resources 2014, update 2015: International soil classification system for naming soils and creating soil maps*. World Soil Resources Report, 106, Rome: Food and Agriculture Organization of the United Nations (FAO).

Jetten, V., Govers, G., & Hessel, R. (2003). Erosion models: Quality of spatial predictions. *Hydrological Processes*, *17*, 887–900. https://doi.org/10.1002/hyp.1168

Kuhwald, M., Blaschek, M., Minkler, R., Nazemtseva, Y., Schwanebeck, M., Winter, J., Duttmann, R., & Goss, M. J. (2016). Spatial analysis of long-term effects of different tillage practices based on penetration resistance. *Soil Use and Management*, *32*, 240–249. https://doi.org/10.1111/sum.12254

Kuhwald, M., Hamer, W. B., Saggau, P., Augustin, K., & Duttmann, R. (2020). Advances in dynamic Modelling of landscape processes: The example of soil compaction. *GEOÖKO*, *41*(1-2), 95–114.

Lal, R. (2014). Desertification and soil erosion. *Global environmental change*. Cham: Springer. https://doi.org/10.1007/978-94-007-5784-4_7

Ledermann, T., Herweg, K., Liniger, H. P., Schneider, F., Hurni, H., & Prasuhn, V. (2010). Applying erosion damage mapping to assess and quantify off-site effects of soil erosion in Switzerland. *Land Degradation & Development*, *21*, 353–366. https://doi.org/10.1002/ldr.1008

Leguédois, S., & Le Bissonnais, Y. (2004). Size fractions resulting from an aggregate stability test, interrill detachment and transport. *Earth Surface Processes and Landforms*, *29*, 1117–1129. https://doi.org/10.1002/esp.1106

Luetzenburg, G., Bittner, M. J., Calsamiglia, A., Renschler, C. S., Estrany, J., & Poeppl, R. (2020). Climate and land use change effects on soil erosion in two small agricultural catchment systems Fugnitz - Austria, Can Revull - Spain. *The Science of the Total Environment*, *704*, 1–15. https://doi.org/10.1016/j.scitotenv.2019.135389

LVermGeo. (2005–2007). ©GeoBasis_DE/LVermGeoSH: Digital elevation model (1x1 m).

LVermGeo. (2017). ©GeoBasis_DE/LVermGeoSH: Digital orthofoto.

Martinez-Agirre, A., Álvarez-Mozos, J., Milenković, M., Pfeifer, N., Giménez, R., Valle, J. M., & Rodríguez, Á. (2020). Evaluation of terrestrial laser scanner and structure from motion photogrammetry techniques for quantifying soil surface roughness parameters over agricultural soils. *Earth Surface Processes and Landforms*, *45*, 605–621. https://doi.org/10.1002/esp.4758

McBratney, A. B., Mendonça Santos, M. L., & Minasny, B. (2003). On digital soil mapping. *Geoderma*, *117*, 3–52. https://doi.org/10.1016/S0016-7061(03)00223-4

McBratney, A. B., Odeh, I. O. A., Bishop, T. F. A., Dunbar, M. S., & Shatar, T. M. (2000). An overview of pedometric techniques for use in soil survey. *Geoderma*, *97*, 293–327. https://doi.org/10.1016/S0016-7061(00)00043-4

Merritt, W. S., Letcher, R. A., & Jakeman, A. J. (2003). A review of erosion and sediment transport models. *Environmental Modelling & Software*, *18*, 761–799. https://doi.org/10.1016/S1364-8152(03)00078-1

Michael A, Schmidt J, Schmidt W (eds). (1996). *EROSION 2D - Ein Computermodell zur Simulation der Bodenerosion durch Wasser. Band II: Parameterkatalog*. Freiberg: Sächsische Landesanstalt für Landwirtschaft/Sächsisches Landesamt für Umwelt und Geologie.

Millares, A., Gulliver, Z., & Polo, M. J. (2012). Scale effects on the estimation of erosion thresholds through a distributed and physically-based hydrological model. *Geomorphology*, *153–154*, 115–126. https://doi.org/10.1016/j.geomorph.2012.02.016

Moloney, T., Fenton, O., & Daly, K. (2020). Ranking connectivity risk for phosphorus loss along agricultural drainage ditches. *The Science of the Total Environment*, *703*, 134556. https://doi.org/10.1016/j.scitotenv.2019.134556

Montgomery, D. R. (2007). Soil erosion and agricultural sustainability. *Proceedings of the National Academy of Sciences of the United States of America*, *104*, 13268–13272. https://doi.org/10.1073/pnas.0611508104

Mosimann, T., Sanders, S., & Brunotte, J. (2008). Erosion protection in tractor tracks. *Landtech*, *1*, 20–21. https://doi.org/10.15150/lt.2008.761

NAW (Normenausschuss Wasserwesen) 2002. DIN ISO 11277:2002-08, Bodenbeschaffenheit_- Bestimmung der Partikelgrößenverteilung in Mineralböden_- Verfahren mittels Siebung und Sedimentation (ISO_11277:1998_+ ISO_11277:1998 Corrigendum_1:2002). Berlin: Verlag GmbH- 13.080.99(19707).

Parker, D. B., Michel, T. G., & Smith, J. L. (1995). Compaction and water velocity effects on soil erosion in shallow flow. *Journal of Irrigation and Drainage Engineering*, *121*, 170–178. https://doi.org/10.1061/(ASCE)0733-9437(1995)121:2(170)

Parsons, A. J. (2019). How reliable are our methods for estimating soil erosion by water? *The Science of the Total Environment*, *676*, 215–221. https://doi.org/10.1016/j.scitotenv.2019.04.307

Peel, M. C., Finlayson, B. L., & McMahon, T. A. (2007). Updated world map of the Köppen-Geiger climate classification. *Hydrology and Earth System Sciences*, *11*, 1633–1644. https://doi.org/10.5194/hess-11-1633-2007

Pennock, D. (2019). *Soil erosion: The greatest challenge for sustainable soil management*: Rome: FAO.

Poesen, J. (2018). Soil erosion in the Anthropocene: Research needs. *Earth Surface Processes and Landforms*, *43*, 64–84. https://doi.org/10.1002/esp.4250

Poesen, J., Nachtergaele, J., Verstraeten, G., & Valentin, C. (2003). Gully erosion and environmental change: Importance and research needs. *Gully Erosion and Global Change*, *50*, 91–133. https://doi.org/10.1016/S0341-8162(02)00143-1

Poppenga, S. K., & Worstell, B. B. (2016). Hydrologic connectivity: Quantitative assessments of hydrologic-enforced drainage structures in an elevation model. *Journal of Coastal Research*, *76*, 89–106. https://doi.org/10.2112/SI76-009

Prasuhn, V. (2011). Soil erosion in the Swiss Midlands: Results of a 10-year field survey. *Geomorphology*, *126*, 32–41. https://doi.org/10.1016/j.geomorph.2010.10.023

Prasuhn, V. (2020). Twenty years of soil erosion on-farm measurement: Annual variation, spatial distribution and the impact of conservation programmes for soil loss rates in Switzerland. *Earth Surface Processes and Landforms*, *37*, 1539–1554. https://doi.org/10.1002/esp.4829

Remund, D., Liebisch, F., Liniger, H. P., Heinimann, A., & Prasuhn, V. (2021). The origin of sediment and particulate phosphorus inputs into water bodies in the Swiss Midlands – A twenty-year field study of soil erosion. *Catena*, *203*, 105290. https://doi.org/10.1016/j.catena.2021.105290

Rieger, W. (1998). A phenomenon-based approach to upslope contributing area and depressions in DEMs. *Hydrological Processes*, *12*, 857–872. https://doi.org/10.1002/(SICI)1099-1085(199805)12:6%3C857:AID-HYP659%3E3.0.CO;2-B

Routschek, A., Schmidt, J., & Kreienkamp, F. (2014). Impact of climate change on soil erosion — A high-resolution projection on catchment scale until 2100 in Saxony/Germany. *Catena*, *121*, 99–109. https://doi.org/10.1016/j.catena.2014.04.019

Saggau, P., Bug, J., Gocht, A., & Kruse, K. (2017). Aktuelle bodenerosionsgefährdung durch wind und wasser in Deutschland. *Bodenschutz*, *17*, 120–125. https://doi.org/10.37307/j.1868-7741.2017.04.04

Saggau, P., Kuhwald, M., & Duttmann, R. (2019). Integrating soil compaction impacts of tramlines into soil erosion modelling: A field-scale approach. *Soil Systems*, *3*, 51. https://doi.org/10.3390/soilsystems3030051

Schindewolf, M., & Schmidt, J. (2012). Parameterization of the EROSION 2D/3D soil erosion model using a small-scale rainfall simulator and upstream runoff simulation. *Catena*, *91*, 47–55. https://doi.org/10.1016/j.catena.2011.01.007

Schindewolf, M., Schmidt, J., & Von Werner, M. (2012). Modeling soil erosion and resulting sediment transport into surface water courses on regional scale. *Zeitschrift für Geomorphologie, Supplementary Issues*, *57*, 157–175. https://doi.org/10.1127/0372-8854/2012/S-00087

Schindewolf, M., Schmidt, J., & Von Werner, M. (2013). Modeling soil erosion and resulting sediment transport into surface water courses on regional scale. *ZfG Supplementary Issues*, *57*, 157–175. https://doi.org/10.1127/0372-8854/2012/S-00087

Schmidt, J. (1991). A mathematical model to simulate rainfall erosion. In erosion, transport and deposition processes—Theories and models. H.-R. Bork, J. de Poley & A. P. Schick, *Erosion, transport and deposition processes*. 19, 101–109. Catena Supplements.

Schmidt, J. (1992). Modelling long-term soil loss and landform change. *Overland flow*. UCL Press.

Schmidt, J. (1996). Entwicklung und Anwendung eines physikalisch begründeten Simulationsmodells für die Erosion geneigter landwirtschaftlicher Nutzflüchen. *Berliner geographische Abhandlungen*, *61*, 152 S. https://doi.org/10.23689/fidgeo-3199.

Schmidt, J., Von Werner, M., & Michael, A. (1999). Application of the EROSION 3D model to the Catsop watershed, The Netherlands. *Catena*, *37*, 449–456. https://doi.org/10.1016/S0341-8162(99)00032-6

Shi, P., Arter, C., Liu, X., Keller, M., & Schulin, R. (2017). Soil aggregate stability and size-selective sediment transport with surface runoff as affected by organic residue amendment. *The Science of the Total Environment*, *607–608*, 95–102. https://doi.org/10.1016/j.scitotenv.2017.07.008

Silgram, M., Jackson, D. R., Bailey, A., Quinton, J., & Stevens, C. (2010). Hillslope scale surface runoff, sediment and nutrient losses associated with tramline wheelings. *Earth Surface Processes and Landforms*, *59*, 699–706. https://doi.org/10.1002/esp.1894

Starkloff, T., & Stolte, J. (2014). Applied comparison of the erosion risk models EROSION 3D and LISEM for a small catchment in Norway. *Catena*, *118*, 154–167. https://doi.org/10.1016/j.catena.2014.02.004

Steinhoff-Knopp, B., & Burkhard, B. (2018). Soil erosion by water in Northern Germany: Long-term monitoring results from lower Saxony. *Catena*, *165*, 299–309. https://doi.org/10.1016/j.catena.2018.02.017

ten Damme, L., Stettler, M., Pinet, F., Vervaet, P., Keller, T., Munkholm, L. J., & Lamandé, M. (2019). The contribution of tyre evolution to the reduction of soil compaction risks. *Soil and Tillage Research*, *194*, 104283. https://doi.org/10.1016/j.still.2019.05.029

M Von Werner (ed). 2007. Erosion-3D: Benutzerhandbuch. Ver. 3.015: Berlin.

M Von Werner (ed). 2009. Datenbank-Prozessor: Benutzerhandbuch. Ver. 1.80: Berlin.

Walker, S. J., Dijk, A. I. J. M., Wilkinson, S. N., & Hairsine, P. B. (2021). A comparison of hillslope drainage area estimation methods using high-resolution DEMs with implications for topographic studies of gullies. *Earth Surface Processes and Landforms*, *46*, 2229–2247. https://doi.org/10.1002/esp.5171

Wang, L., & Liu, H. (2006). An efficient method for identifying and filling surface depressions in digital elevation models for hydrologic analysis and modelling. *International Journal of Geographical Information Science*, *20*, 193–213. https://doi.org/10.1080/13658810500433453

Weisskopf, P., Reiser, R., Rek, J., & Oberholzer, H.-R. (2010). Effect of different compaction impacts and varying subsequent management practices on soil structure, air regime and microbiological parameters. *Soil and Tillage Research*, *111*, 65–74. https://doi.org/10.1016/j.still.2010.08.007

Wilken, F., Baur, M., Sommer, M., Deumlich, D., Bens, O., & Fiener, P. (2018). Uncertainties in rainfall kinetic energy-intensity relations for soil erosion modelling. *Catena*, *171*, 234–244. https://doi.org/10.1016/j.catena.2018.07.002

Withers, P. J. A., Hodgkinson, R. A., Bates, A., & Withers, C. M. (2006). Some effects of tramlines on surface runoff, sediment and phosphorus mobilization on an erosion-prone soil. *Soil Use and Management*, *22*, 245–255. https://doi.org/10.1111/j.1475-2743.2006.00034.x

How to cite this article: Saggau, P., Kuhwald, M., Hamer, W. B., & Duttmann, R. (2022). Are compacted tramlines underestimated features in soil erosion modeling? A catchment-scale analysis using a process-based soil erosion model. *Land Degradation & Development*, *33*(3), 452–469. https://doi.org/10.1002/ldr.4161